

## MANEUVER DESIGN OVERVIEW OF THE 2018 INSIGHT MARS LANDER MISSION

**Min-Kun Chung,<sup>\*</sup> Yungsun Hahn,<sup>†</sup> C. Allen Halsell,<sup>‡</sup> Sarah Elizabeth McCandless,<sup>§</sup> Evgeniy Sklyanskiy,<sup>\*\*</sup> and Mark Wallace<sup>††</sup>**

Launched on May 5, 2018, the Interior Exploration using Seismic Investigations, Geodesy, and Heat Transport (InSight) spacecraft landed safely on Mars on November 26, 2018. To deliver the lander accurately to the landing site, six trajectory correction maneuvers (TCMs) were planned along the reference trajectory from Earth launch to Mars entry. For the last two TCMs, there were two corresponding contingency TCMs planned that could be executed in the event that the corresponding nominal one failed. There were also twenty pre-designed menu TCMs available for execution at the time of the last contingency TCM, about 8 hours before the Mars entry, descent, and landing. This navigation paper overviews the maneuver design of each TCM, as well as how each one actually performed during operations.

### INTRODUCTION

The Interior Exploration using Seismic Investigations, Geodesy, and Heat Transport (InSight) spacecraft was launched on May 5, 2018, the first day of the scheduled launch period. On November 26, 2018, the InSight lander safely landed on Mars. The navigation objective was to deliver the lander to a relatively flat landing site in the Elysium Planitia region on Mars. The pre-launch reference trajectory was designed to achieve this objective.<sup>1</sup> However, deviations from the nominal are inevitable and their causes are numerous, for example: launch vehicle injection errors, hard-to-predict small forces such as spacecraft outgassing, anomalies such as spacecraft entering safe-mode, and maneuver execution errors especially during the time near the Entry, Descent, and Landing (EDL). The Orbit Determination (OD) process solves for the estimates of the current spacecraft states and uncertainties together with the propagation model to predict the future flight path and maps the associated uncertainties. It is then the goal of Flight Path Control

---

<sup>\*</sup> Mission Design Engineer, Mission Design and Navigation Section, Jet Propulsion Laboratory, California Institute of Technology, M/S 264-820, 4800 Oak Grove Drive, Pasadena, CA. 91109.

<sup>†</sup> Navigation Engineer, Mission Design and Navigation Section, Jet Propulsion Laboratory, California Institute of Technology, M/S 264-820, 4800 Oak Grove Drive, Pasadena, CA. 91109.

<sup>‡</sup> InSight Navigation Team Chief, Mission Design and Navigation Section, Jet Propulsion Laboratory, California Institute of Technology, M/S 264-820, 4800 Oak Grove Drive, Pasadena, CA. 91109.

<sup>§</sup> Navigation Engineer, Mission Design and Navigation Section, Jet Propulsion Laboratory, California Institute of Technology, M/S 264-820, 4800 Oak Grove Drive, Pasadena, CA. 91109.

<sup>\*\*</sup> Mission Design Engineer, Mission Design and Navigation Section, Jet Propulsion Laboratory, California Institute of Technology, M/S 198-326, 4800 Oak Grove Drive, Pasadena, CA. 91109.

<sup>††</sup> Mission Design Engineer, Mission Design and Navigation Section, Jet Propulsion Laboratory, California Institute of Technology, M/S 264-850, 4800 Oak Grove Drive, Pasadena, CA. 91109.

(FPC) to design Trajectory Correction Maneuvers (TCMs) to place the spacecraft back on its course to target the landing site. This navigation paper overviews the maneuver design of each TCM, as well as how each one actually performed during navigation operations.

### Introduction to TCMs

Figure 1 shows six TCMs (marked by numbers 1-6 in black) along the reference trajectory (black) from Earth launch to Mars entry in EME2000. In the baseline, TCM-1 had a deterministic component as the result of trajectory optimization for the given launch and arrival conditions; it also corrects the injection errors. The rest of the TCMs (TCM-2 to 6) were planned to be all statistical; they correct any previous TCM execution errors, as well as any OD errors. A thruster calibration (TCAL) was scheduled between TCM-1 and TCM-2, which was another possible source of error. In addition, contingency maneuvers were scheduled for each of the last two TCMs, namely TCM-5X and TCM-6X, respectively. These contingency maneuvers would have been executed if the corresponding nominal one had failed to execute. Finally, a menu of twenty contingency maneuvers (labeled TCM-6XM) were pre-designed and pre-verified for execution at the time of TCM-6X, if the Project deemed it necessary due to a safing event or other anomaly.

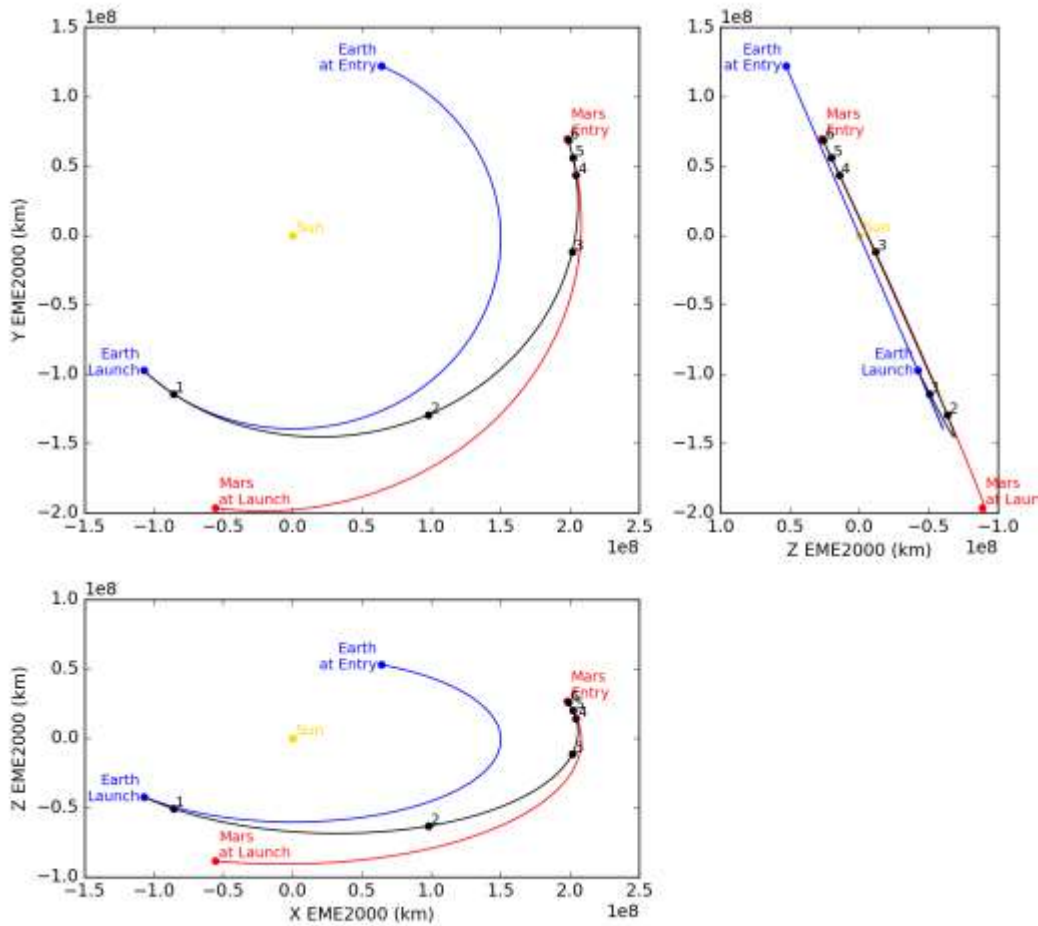


**Figure 1. InSight Reference Trajectory from Launch to Entry in EME2000.** Earth is in blue, Mars in red, and InSight in black. TCM numbers are in black.

## Introduction to TCM Targets and Requirements

Although the reference trajectory appears relatively simple and direct with no flybys, its final targets are not the B-plane targets as in an orbital mission but rather the landing site location (latitude and longitude) after EDL, which adds complexity to the maneuver design and delivery. The prelaunch landing site location was  $4.46^\circ$  latitude and  $135.97^\circ$  E longitude. Early in cruise it was slightly updated to  $4.51^\circ$  latitude and  $135.99^\circ$  E longitude by Project decision.

Given the atmosphere and wind models, the landing site location translates into the entry targets, where the entry state is defined by the incoming reference trajectory at a 3,522.2 km radius from Mars; this is the first component of the entry target. The second entry target is the entry flight path angle (EFPA), with an EDL requirement of  $-12.0^\circ \pm 0.21^\circ$  ( $3\text{-}\sigma$ ). A third target parameter is necessary for a TCM search. We chose the B-plane theta angle<sup>\*</sup>; however, another independent parameter would have worked just as well, for example, the entry flight path azimuth.

The entry time was required to be reasonably fixed to support communication relay by MRO and the two MarCO spacecraft at entry. However, targeting a fixed landing site for a TCM search produces a change in the entry time whenever the atmosphere model or the wind model changes. Thus, to avoid any unnecessary changes in the entry time whenever the models change, a slightly updated set of landing targets were generated instead to preserve a relatively constant entry time.<sup>2</sup>

Also, it is noted that there was a minimum maneuver magnitude of 40 mm/s for any TCM. For TCM magnitudes less than 40 mm/s, there were options to increase it to the minimum 40 mm/s deliberately by slightly adjusting the EFPA or the entry time.<sup>†</sup>

## MANEUVER DESIGN CYCLES

FPC interacts with OD and Guidance and Control (GNC) in a TCM design cycle.

### Interface with OD

An OD solution is delivered internally in the form of files. Those of interest to FPC include the following: (1) the constants including the maneuver times, etc.; (2) the binary file including the propagation and estimation models; (3) the trajectory file; and (4) the mapping results of the various parameters to the future times. For every OD solution, FPC designs a TCM that achieves the entry and landing targets. In addition, a statistical analysis is initiated based on the current OD mapping and completed based on the nominal TCM mapping<sup>‡</sup> to the entry.

### Interface Cycle with GNC

As the data cutoff (DCO) for a TCM approaches, OD delivers a preliminary OD solution; FPC generates a corresponding TCM solution with an impulse burn in the form of a Maneuver Profile File (MPF) that contains the maneuver magnitude and direction in EME2000 coordinates. The preliminary MPF is delivered to GNC. GNC, in turn, delivers a Maneuver Performance Data File (MPDF) that contains the thrust and mass flow rate information of the thrusters. FPC uses the MPDF to design a finite burn that achieves the entry and landing targets. When a final OD solution is delivered at the DCO, FPC designs a final, finite burn and delivers a final MPF to GNC.

---

\* The B-plane theta angle is also what InSight DSENDS returned for the corrected or estimated parameter to target a specified landing site (See the EDL sub-section under the MANEUVER DESIGN TOOLS section below).

† For more details refer to the sub-section, TCM Search, under the MANEUVER DESIGN TOOLS section below.

‡ The nominal TCM mapping is based on the prelaunch covariance study. For more details refer to Covariance Analysis Filter Assumptions in Reference 1.

GNC in turn delivers a Maneuver Implementation File (MIF) that contains information on a sequence of turns, burns, and slews to implement the designed TCM, and the corresponding error covariances. FPC verifies the MIF, as well as a couple of configuration files to be uploaded to the spacecraft for execution.

## MANEUVER DESIGN TOOLS

DSENDS (Dynamics Simulator for Entry, Descent and Surface landing)<sup>\*</sup> was used for EDL. Monte (Mission Analysis, Operations, and Navigation Toolkit Environment)<sup>†</sup> was used for the main maneuver design and analysis.

### Interface to EDL

Given an atmosphere model and a wind model, InSight DSENDS operates in the following two modes: (1) simply propagate the specified entry time and state onto the surface; or (2) propagate the specified entry time and state with the specified EFPA to return the corrected entry time and the corrected B-plane angle that will target the specified landing location. The second mode was essential in implementing a TCM search to determine an entry state with the specified EFPA that targets the specified landing location on the surface by running DSENDS iteratively until convergence.

### TCM Search

The second DSENDS mode was used to search for a TCM that resulted in a fixed  $-12.0^\circ$  EFPA. As stated briefly before, a TCM search included the three targets at the entry time: radius (3,522.2 km), EFPA ( $-12.0^\circ$ ), and B-plane theta. For a free EFPA solution, a set of EFPA values around the nominal  $-12.0^\circ$  were used to run DSENDS in parallel to construct interpolated functions of the entry targets with respect to EFPA. A few dozen EFPA points strategically located around  $-12.0^\circ$ , more densely packed closer to the center, yielded a decent interpolation only on the order of several meters when mapped onto the surface. These interpolated functions were used to compute either the minimum possible  $\Delta V$  solution or the 40 mm/s minimum implementable solution closest to the nominal  $-12.0^\circ$  EFPA, which resulted in a smaller entry time bias.

### Statistical Analysis

For statistical maneuver analysis Monte LAMBIC (Linear Analysis of Maneuvers with Bounds and Inequality Constraints) was used. Three modes of simulation were used: Prelaunch, Fixed, and Injection.

*Prelaunch Mode.* The prelaunch  $\Delta V$  analysis was performed with an injection covariance representing the initial spacecraft position and velocity uncertainties at TIP (Target Interface Point). In this mode, an OD error from a covariance study was added to each injection sample in order to generate a  $\Delta V$  design. The design differs for each sample, and an execution error is also added. Each maneuver sample contains errors from three sources: injection, OD, and execution. (See Reference 1 for the tabulated statistical  $\Delta V$  results, the maneuver execution error model, and the covariance analysis filter assumptions.)

*Fixed Mode.* As real data are processed after launch, the normal procedure is to switch to a mid-mission method, which “fixes” the upcoming maneuver design based on the best OD estimate, which is treated as if it was a true state, while passing the OD uncertainties to the down-

---

<sup>\*</sup> <https://dshell.jpl.nasa.gov/DSENDS/>

<sup>†</sup> <https://montepy.jpl.nasa.gov/>

stream maneuvers. The commanded  $\Delta V$  is the same for all the samples in this simulation mode. The dispersion comes from execution errors only. The movement of the best estimate and the reduction in its uncertainties at later DCO dates are not factored in this mode; it does not account for future development (in size and direction) expected before the final design.

*Injection Mode.* In order to address this deficiency in the Fixed Mode analysis, the statistical  $\Delta V$  analysis script was enhanced with a new mode such that the current OD covariance can be treated as a re-injection. This enhancement proved very useful during operations, when larger-than-expected out-gassing and the thrusting to counteract it made OD uncertainties much larger than what was assumed by the prelaunch  $\Delta V$  analysis. Then as the OD uncertainties leveled off and were not decreasing any more, the simulation was switched from the Injection to Fixed Mode. The Injection Mode was also useful when assessing the  $\Delta V$  cost of the next TCM if the current TCM were to be canceled, since the OD uncertainties were expected to further decrease before the next TCM.

## **Presentation**

To communicate the maneuver design options to the NAG (Navigation Advisory Group) and the Project, each TCM option as well as the detailed TCM information had to be presented. Most presentation slides were automatically generated by scripts.\*

*Maneuver Options Table.* A one-page maneuver options table turned out to be quite effective in communicating the available maneuver options, especially for the later TCMs when the options included a free EFPA solution, as well as the option of canceling the TCM. The first column of the table was always the OD-only without any TCM. Usually the four TCM solutions included the following options: (1) the current TCM with the fixed EFPA; (2) the current TCM with the free EFPA; (3) the next TCM (w/o the current) with the fixed EFPA; and (4) the next TCM (w/o the current) with the free EFPA. The rows were grouped into a few different information categories: TCM option,  $\Delta V$ , B-plane, entry, and landing. For example, Table 1 shows the maneuver options at TCM-4. The TCM-4 fixed EFPA solution is less than 40 mm/s (Option 1), while the TCM-4 free EFPA solution is feasible at 40 mm/s with about a 6 second entry time bias (Option 2). The TCM-5 fixed EFPA solution without TCM-4 seemed just as good as TCM-4 delivery without the entry time bias (Option 3) as well as the TCM-5 free EFPA solution (Option 4).

*Detailed Maneuver Information Slide.* The rest of the presentation consisted of the detailed information on each maneuver option: the text output of the detailed maneuver summary, the burn geometry plot, the station allocation plot, the Doppler shift plot, the statistical analysis table (for example, Table 2 below), the B-plane delivery ellipse plot (for example, Figure 2 below), and the  $\Delta V$  and  $\Delta \text{EntryTime}$  vs EFPA plot (for example, Figure 4 below) for the free EFPA solution.

---

\* Python-pptx was used for slide generation. See <https://python-pptx.readthedocs.io/en/latest/>.

**Table 1. A Sample Maneuver Options Table.** TCM-4 Options Table showing a fixed EFPA TCM-4 solution below 40 mm/s and a free EFPA TCM-4 solution raising the TCM magnitude to 40 mm/s as well as the TCM-5 solutions without TCM-4.

Option	0	1	2	3	4
TCM	No Burn	TCM-4	TCM-4	TCM-5	TCM-5
FPA	-	Fixed	Free	Fixed	Free
DVMag (m/s)	-	0.0300	0.0400	0.0560	0.0400
Earth Angle (deg)	-	21.6005	18.0416	21.9589	51.4112
Turn Angle (deg)	-	130.2424	121.3908	126.9604	142.8591
TCM-5 Delivery SMAA (km)	1.211	8.715	8.663	9.589	9.622
SMIA (km)	0.556	8.412	8.420	8.104	6.448
Theta (deg)	115.587	140.672	138.523	80.489	76.307
Entry Time (UTC)	26-NOV-2018 19:38:34.1673	26-NOV-2018 19:39:04.2110	26-NOV-2018 19:39:09.8635	26-NOV-2018 19:39:04.1700	26-NOV-2018 19:38:55.7546
EFPA (deg)	-13.0589	-12.0000	-11.9929	-12.0000	-12.0099
dEntry (sec)	-30.0283	0.0154	5.6679	-0.0256	-8.4410
Landing Time (UTC)	26-NOV-2018 19:44:19.2673	26-NOV-2018 19:45:30.2111	26-NOV-2018 19:45:36.0635	26-NOV-2018 19:45:30.1701	26-NOV-2018 19:45:21.0546
Lat (deg)	3.7597	4.5100	4.5100	4.5100	4.5100
Lon (deg)	133.1434	135.9901	135.9901	135.9900	135.9899
Miss (km)	173.9146	0.0033	0.0050	0.0023	0.0037

## MANEUVER PERFORMANCE DURING OPERATIONS

In this section we summarize each TCM design and its performance during operations.

### TCM-1

The primary purpose of TCM-1 was to remove the injection bias and clean up the injection errors. Due to higher-than-expected out-gassing during the beginning of the cruise, OD was not as stable as expected at the nominal TCM-1 date at Launch+10d. The Project made a decision to delay its execution by one week to L+17d, since the  $\Delta V$  magnitude vs TCM-1 date plot remained relatively flat for the first couple of weeks. Also, a two-maneuver re-optimization strategy combining TCM-1 and TCM-2 was adopted over a single TCM-1 design. This strategy of splitting the cost had two advantages. First, the sum of the two  $\Delta V$  magnitudes (3.777 m/s and 0.939 m/s) was less than a single TCM-1  $\Delta V$  (4.845 m/s) (note that even the single TCM-1 value is below the prelaunch mean of 7.101 m/s because of the good injection). Second, the intermediate aimpoint of TCM-1 was outside of the B-plane impact radius at Mars, such that the cumulative impact probability ( $0.744e-03$ ) was less than the requirement ( $1.e-02$ ). The single TCM-1 case was  $1.044e-02$ . In addition, the uncertainty in the TCAL maneuver between TCM-1 and TCM-2 made the case stronger to perform the 2-maneuver optimization. The statistical  $\Delta V$ s are tabulated in Table 2, and the B-plane deliveries are depicted in Figure 2.

**Table 2. Statistical  $\Delta V$  for TCM-1.**

TCM	Epoch (UTC)	DV Mean (m/s)	DV Sigma (m/s)	DV01 (m/s)	DV50 (m/s)	DV99 (m/s)
OD	15-MAY-2018 15:29:46	0.000	0.000	0.000	0.000	0.000
<b>TCM-1</b>	<b>22-MAY-2018 18:00:00</b>	<b>3.779</b>	<b>0.027</b>	<b>3.715</b>	<b>3.779</b>	<b>3.843</b>
TCAL	26-JUN-2018 20:10:00	0.473	0.030	0.401	0.473	0.542
<b>TCM-2</b>	<b>28-JUL-2018 18:00:00</b>	<b>1.033</b>	<b>0.164</b>	<b>0.713</b>	<b>1.018</b>	<b>1.522</b>
TCM-3	12-OCT-2018 18:00:00	0.071	0.036	0.016	0.064	0.177
TCM-4	11-NOV-2018 18:00:00	0.062	0.025	0.015	0.059	0.129
TCM-5	18-NOV-2018 18:00:00	0.042	0.017	0.009	0.040	0.089
TCM-6	25-NOV-2018 21:40:00	0.173	0.076	0.039	0.162	0.382
<b>Total</b>		<b>5.632</b>	<b>0.200</b>	<b>5.214</b>	<b>5.615</b>	<b>6.211</b>

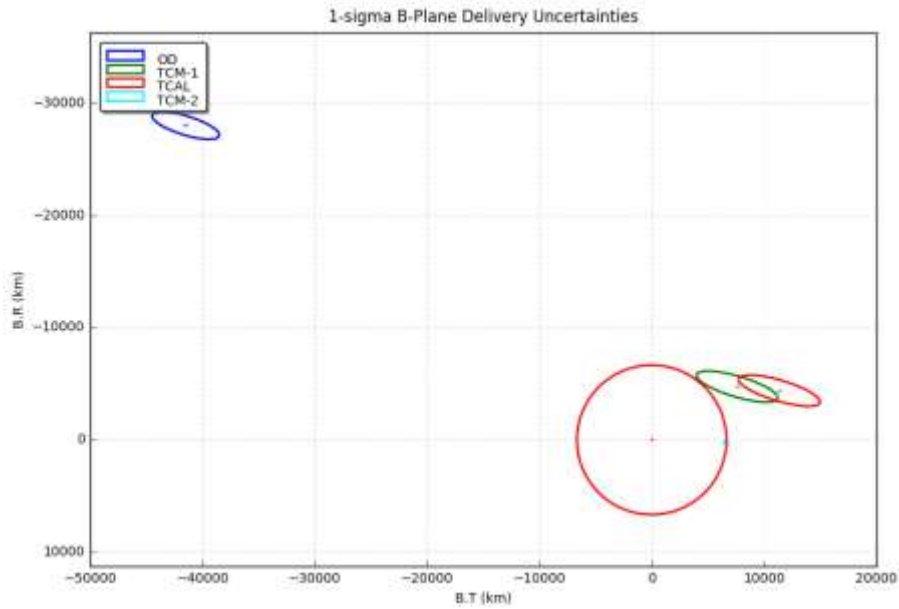


**Figure 2. B-Plane Delivery Ellipses for TCM-1.**

### TCM-2

TCM-2 targeted the entry targets from the reference trajectory, see Figure 3. As the result of TCAL post TCM-1, the TCM-2 design (1.498 m/s) in Table 3 was larger than the mean (1.033 m/s) predicted at TCM-1 design as shown in Table 2 above. It was close to the 99% prediction of 1.522 m/s.

**Table 3. Statistical  $\Delta V$  for TCM-2.**

TCM	Epoch (UTC)	DV Determ (m/s)	DV Mean (m/s)	DV Sigma (m/s)	DV01 (m/s)	DV50 (m/s)	DV99 (m/s)
OD	23-JUL-2018 15:28:44	0.000	0.000	0.000	0.000	0.000	0.000
<b>TCM-2</b>	<b>28-JUL-2018 18:00:00</b>	<b>1.498</b>	<b>1.498</b>	<b>0.014</b>	<b>1.466</b>	<b>1.498</b>	<b>1.529</b>
TCM-3	12-OCT-2018 18:00:00	0.000	0.143	0.063	0.032	0.135	0.315
TCM-4	11-NOV-2018 18:00:00	0.000	0.062	0.025	0.015	0.059	0.130
TCM-5	18-NOV-2018 18:00:00	0.000	0.041	0.016	0.011	0.040	0.088
TCM-6	25-NOV-2018 21:40:00	0.000	0.173	0.075	0.038	0.165	0.374
<b>Total</b>		<b>1.498</b>	<b>1.917</b>	<b>0.106</b>	<b>1.700</b>	<b>1.908</b>	<b>2.189</b>

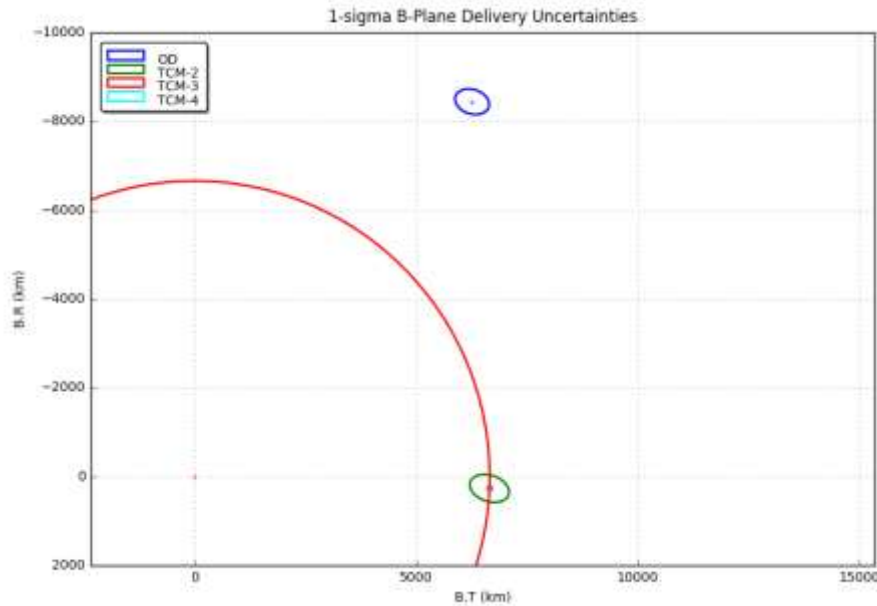


**Figure 3. B-Plane Delivery Ellipses for TCM-2.**

### TCM-3

After TCM-2, the design of TCM-3 with a new OD delivery to the entry targets obtained from the previously delivered reference trajectory started to show some nontrivial differences in the latitude and longitude when the trajectory was propagated to the surface via DSENDS. At this point, the maneuver team built the EDL interface function outlined in the previous section to refine the entry time and targets (primarily the B-plane theta angle for TCM-3). With this fine-tuning, the propagation to the surface resulted in negligible differences in the landing site. The TCM-3 design magnitude was 0.167 m/s, which was slightly larger than the mean 0.143 m/s predicted at the time of TCM-2 design shown in Table 3. We note that by this time the maneuver design scripts were streamlined to produce a complete set of maneuver design products including the presentation package.

**Table 4. Statistical  $\Delta V$  for TCM-3.**

TCM	Epoch (UTC)	DV Determ (m/s)	DV Mean (m/s)	DV Sigma (m/s)	DV01 (m/s)	DV50 (m/s)	DV99 (m/s)
OD	07-OCT-2018 14:32:54	0.000	0.000	0.000	0.000	0.000	0.000
TCM-3	12-OCT-2018 18:00:00	0.167	0.168	0.009	0.147	0.168	0.190
TCM-4	11-NOV-2018 18:00:00	0.000	0.062	0.026	0.014	0.059	0.134
TCM-5	18-NOV-2018 18:00:00	0.000	0.041	0.016	0.010	0.040	0.084
TCM-6	25-NOV-2018 21:40:00	0.000	0.170	0.075	0.039	0.162	0.369
Total		0.167	0.442	0.086	0.281	0.434	0.674

**TCM-4**

From TCM-4 (Entry-15d) onward, a short design cycle of one day was scheduled between DCO to maneuver execution as FPC entered a “fine tuning” stage for the entry, where the designed TCM may be as small as the minimum implementable size of 40 mm/s. The  $-12.0^\circ$  fixed EFPA solution for TCM-4 was only 30 mm/s, which was below the minimum. This could have been raised to 40 mm/s by adjusting EFPA to  $-11.993^\circ$  with an entry time bias of 5.7 seconds (Figure 4 below and Table 1 above).

At the time of the TCM-4 design, the predicted TCM-5 design was 56 mm/s in Table 1 above where the maneuver options are summarized. As can be seen from the size of the TCM-4 delivery ellipse in Figure 5, TCM-4 execution errors could make the dispersion even larger than not doing

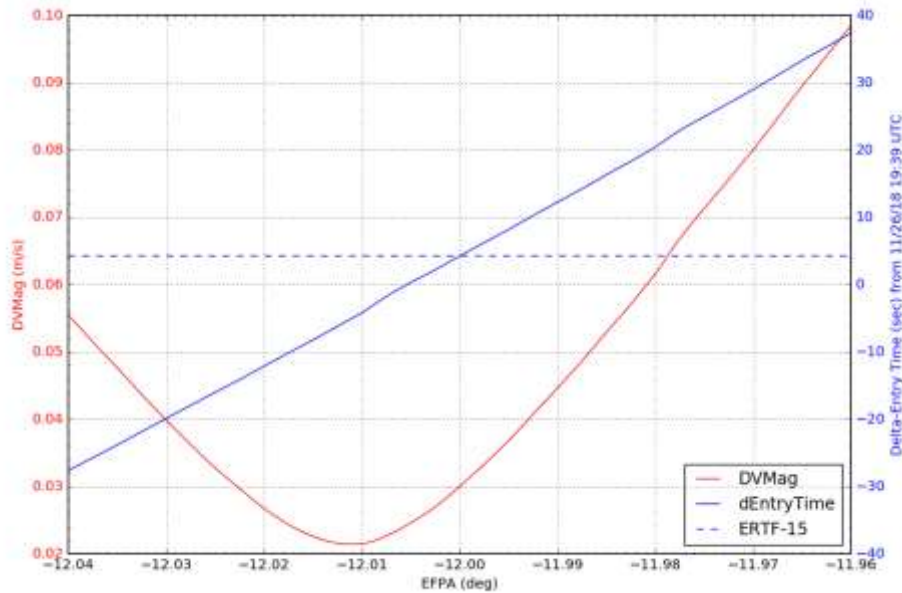


**Figure 4. A Sample  $\Delta V$  and  $\Delta$ EntryTime vs EFPA Plot.** TCM-4 free EFPA solution shows  $\Delta V$  below 40 mm/s at  $-12.0^\circ$  EFPA; however, 40 mm/s can be achieved by adjusting EFPA or  $\Delta$ EntryTime. ERTF-15 is the entry time MRO uses for relay.

TCM-4. Based on all of these factors, TCM-4 was cancelled with the expectation of an accurate OD for the TCM-5 design, with a further hope of canceling TCM-6 at 22 hours before the entry.

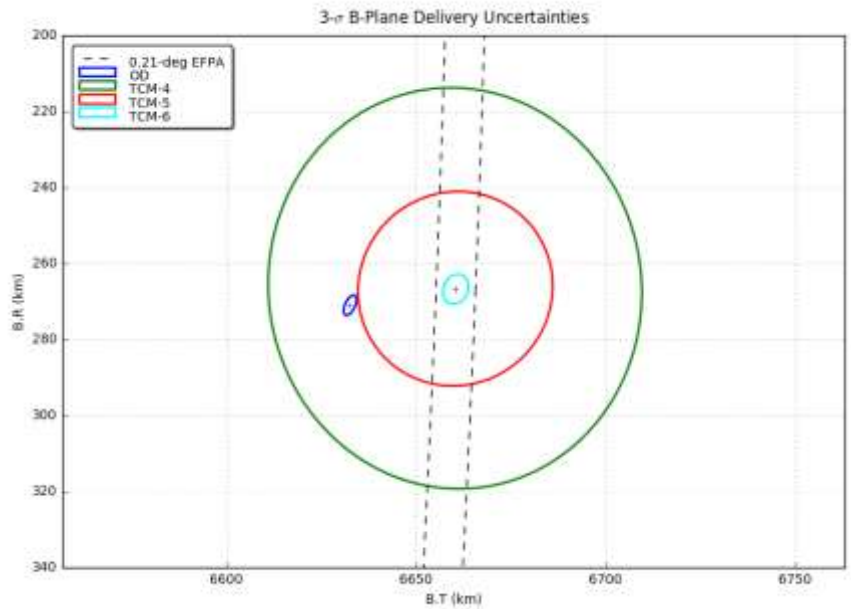


**Figure 5. Delivery Ellipses for TCM-4.**

**TCM-5/TCM-5X**

During the one week following TCM-4 cancellation, the TCM-5 design size remained stable, with a magnitude of about 57 mm/s at DCO. This could have been reduced to 40 mm/s with a small change in EFPA for the benefit of smaller execution errors. However, this option was not adopted since going down to the maneuver limit could make burn-slew decomposition by GNC more difficult. Also considered was the TCM-5X option 3 days later that would result in a smaller delivery error, although the maneuver itself was larger (92 mm/s) as shown in Figure 6. The disadvantage of delaying to TCM-5X was the shortened period (4 vs. 7 days) for reconstructing the maneuver before the critical go/no-go decision for TCM-6. Ultimately, the TCM-5 was executed as designed.

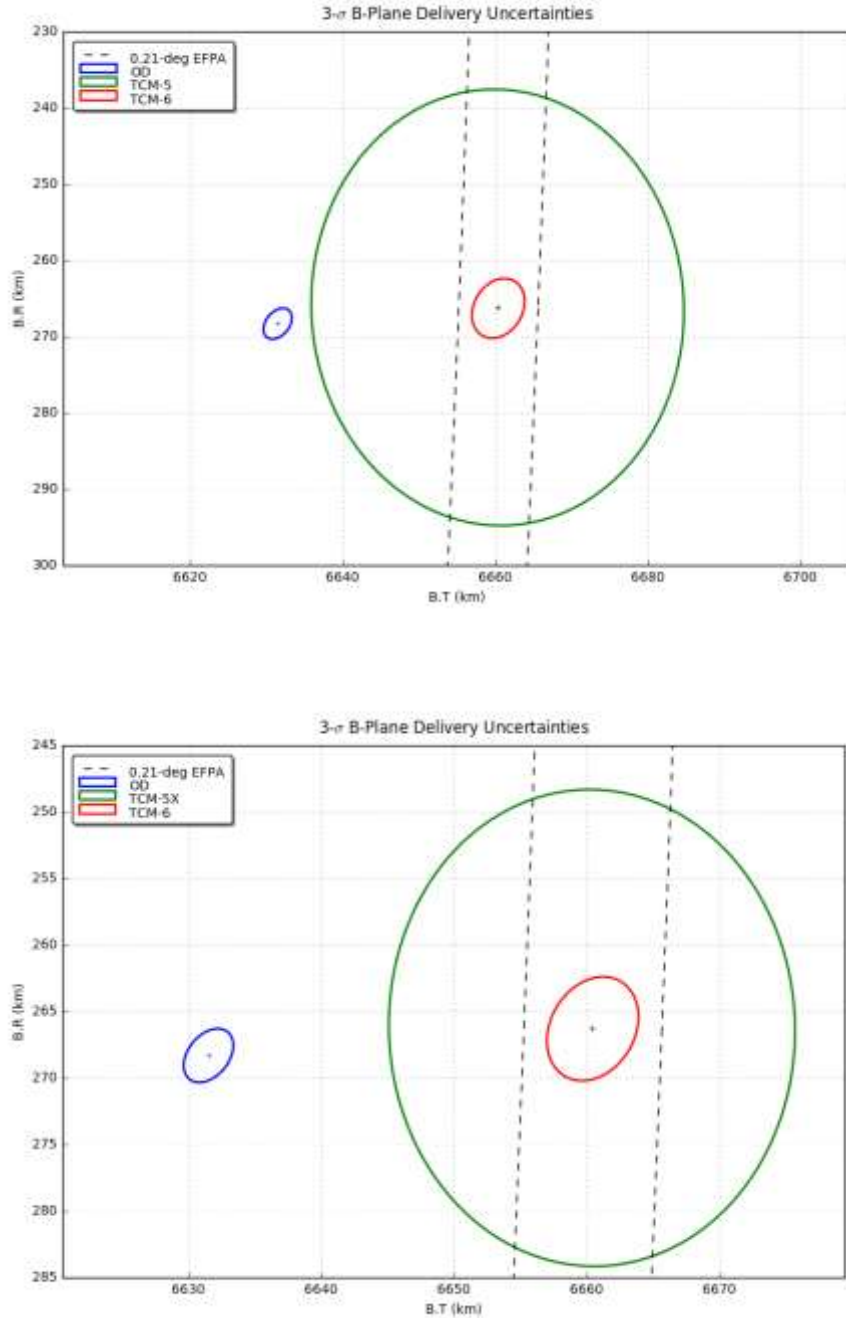


**Figure 6. Delivery Ellipses for TCM-5 (top) and for TCM-5X (bottom).**

### TCM-6/TCM-6X

TCM-5 execution was fairly accurate considering the small maneuver size, leaving the target about  $\sim 7$  km short on the B-plane ( $\sim 20$  km on the surface). The no-TCM6-burn EFPA was  $-11.9^\circ$ , which was acceptable to EDL. From a Navigation perspective, there was no need to perform

TCM-6 as it was yet another small maneuver  $\sim 85$  mm/s with a poor Earth look angle of  $110.08^\circ$ . Furthermore, the spacecraft turn-to-burn angle was  $91.10^\circ$ , which was a difficult angle for GNC to decompose into slew and burn. In addition, the landing site evaluation showed that all the criteria were met by a post-DCO OD right before TCM-6 execution e.g., terrain safety, high fidelity zone by MRO HiRISE instrument, etc.

However, the landing site error on the surface was in the downtrack direction towards a ridged terrain in the north-east. Given the history of previous Mars missions “Landing Long on Mars,”\* the Project elected to proceed with TCM-6 execution. Figure 7 shows the delivery ellipses for TCM-6.

Also, under the circumstance the Project had made a decision not to execute TCM-6X, even in the event that TCM-6 failed to execute.

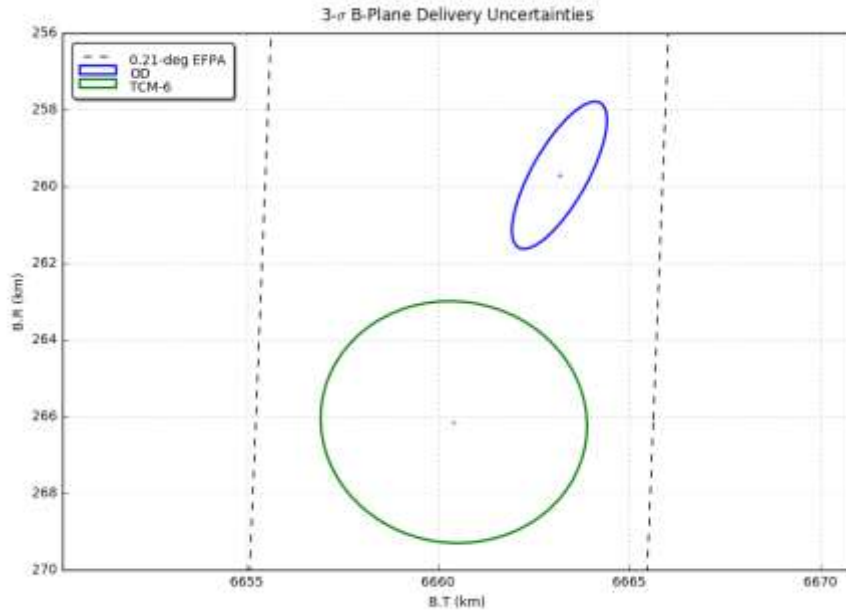


**Figure 7. Delivery Ellipses for TCM-6.**

### TCM Reconstruction Summary

See Table 5 below for a comparison between the TCMs as designed by FPC and as reconstruction by OD and GNC. In particular, TCM-6 was about  $2.3\text{-}\sigma$  off in execution. This TCM-6 execution error as well as the atmospheric uncertainties contributed in InSight coming to rest about 20 km West of the target landing site.

---

\* As it turned out, this was not always the case in the past and InSight was on the opposite side.

**Table 5. TCM Reconstruction Comparison in EME2000**

TCM	Epoch (UTC)	FPC Design			OD Reconstruction			GNC/IMU Reconstruction		
		Mag (m/s)	RA (°)	Dec (°)	Mag (m/s)	RA (°)	Dec (°)	Mag (m/s)	RA (°)	Dec (°)
TCM-1	22-MAY-2018 18:00:00	3.7772	92.0606	-7.8236	3.7612	92.1575	-7.9703	3.7561	91.9105	-8.4321
TCM-2	28-JUL-2018 18:00:00	1.4977	102.2828	-25.8663	1.5030	102.6210	-26.4804	1.4963	102.2720	-26.4348
TCM-3	12-OCT-2018 18:00:00	0.1673	336.3295	61.6730	0.1604	333.4344	61.1926	0.1663	333.4850	60.0395
TCM-4										
TCM-5	18-NOV-2018 18:00:00	0.0571	160.6484	28.2760	0.0634	164.1026	36.1741	0.0616	165.1178	29.3023
TCM-6	25-NOV-2018 21:39:00	0.0850	69.9090	-79.8082	0.0907	92.2825	-78.6892	0.0924	71.6259	-78.0032

**TCM-6XM MENU DESIGN**

Twenty pre-designed (by FPC) and pre-verified (by GNC) menu TCMs were to be available for execution in case TCM-6 failed to execute and TCM-6X (designed at the same time as TCM-6) could not satisfy the landing target requirements. Accordingly, this menu of maneuvers (called TCM-6XM) had to be distributed in such way that the 99% TCM-5 landing dispersion ellipse was reduced to the about size of the 99% TCM-6 landing dispersion ellipse. To accomplish this objective, it was found that clever definition of two rotations could reduce the problem basically into a geometric one.

The first rotation is one that rotates a randomly sampled Gaussian sigma state dispersion from the TCM-5 OD covariance into the “Sigma Frame,” in which the velocity dispersion ( $\delta V$ ) components at TCM-5 DCO are mapped to the landing dispersion ellipse as follows:  $\delta V_x$  very close to the center,  $\delta V_y$  along the semi-major axis, and  $\delta V_z$  along the semi-minor axis. Note that the 3- $\sigma$  position dispersion at TCM-5 DCO maps insignificantly smaller from the center. In addition, an interpolation can be easily obtained from selected DSENDs runs\*, which maps a TCM-5 sigma state dispersion onto the landing dispersion. Figure 8 shows 100,000 randomly sampled TCM-5 sigma dispersions mapped to the landing dispersion together with the landing dispersion ellipses.† The sigma to/from percentage error is computed via 6-D Chi-squared distribution.‡

The second rotation is one that rotates the nominal state at TCM-6XM into the “Velocity Frame,” in which the  $\Delta V$  components at TCM-6XM map the nominal state to the landing dispersion ellipse as follows:  $\Delta V_x$  very close to the center,  $\Delta V_y$  along the semi-major axis, and  $\Delta V_z$  along the semi-minor axis. At TCM-6XM the Velocity Frame turns out to be very close to the frame,§ whose unit vectors are as follows:  $\mathbf{u}_x = \mathbf{r} / |\mathbf{r}|$ ,  $\mathbf{u}_z = \mathbf{r} \wedge \mathbf{v} / |\mathbf{r} \wedge \mathbf{v}|$ , and  $\mathbf{u}_y = \mathbf{u}_z \wedge \mathbf{u}_x$  where  $\mathbf{r}$  and  $\mathbf{v}$  are Mars-centered position and velocity vectors. Figure 8 shows the result of  $\Delta V_y$  (blue) and  $\Delta V_z$  (magenta) at TCM-6XM in the Velocity Frame. Similarly, an interpolation can be easily obtained from selected DSENDs runs\*\*, which maps a TCM-6XM  $\Delta V$  in the Velocity Frame onto the landing dispersion.

---

\* For each TCM dispersion, about 661 runs were made, which took about 5 minutes distributed to 64 CPUs.  
† In a strict sense the landing dispersion is not an ellipse but an elongated ellipse toward the upper-right, down-track direction.  
‡ Implemented by the probability density function, pdf(), and the percent point function, ppf(), of scipy.stats.chi2.  
§ Monte BodyPosDirFrame.  
\*\* For TCM-6XM, about 1681 runs were made for interpolation, which took under 10 minutes distributed to 64 CPUs.

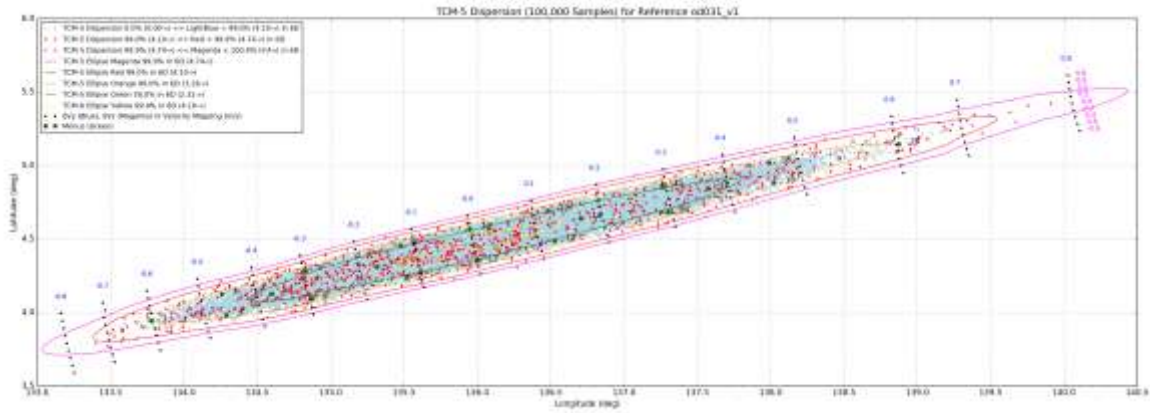


**Figure 8. TCM-5 Landing Dispersion (100,000 Samples from TCM-5 OD Covariance).**

Thus, selecting twenty menu TCMs becomes a matter of distributing a dispersion ellipse of  $\Delta V_y$  by  $\Delta V_z$  size in the Velocity Frame within the 99% TCM-5 dispersion ellipse, for example, as shown in Figure 9. The size of each dispersion ellipse was 0.118 m/s by 0.24 m/s in the Velocity Frame. The  $\Delta V$  “locations” in the Velocity Frame can be converted into EME2000 components for implementation into the MPF, and ultimately into a MIF that is then verified and ready to use.

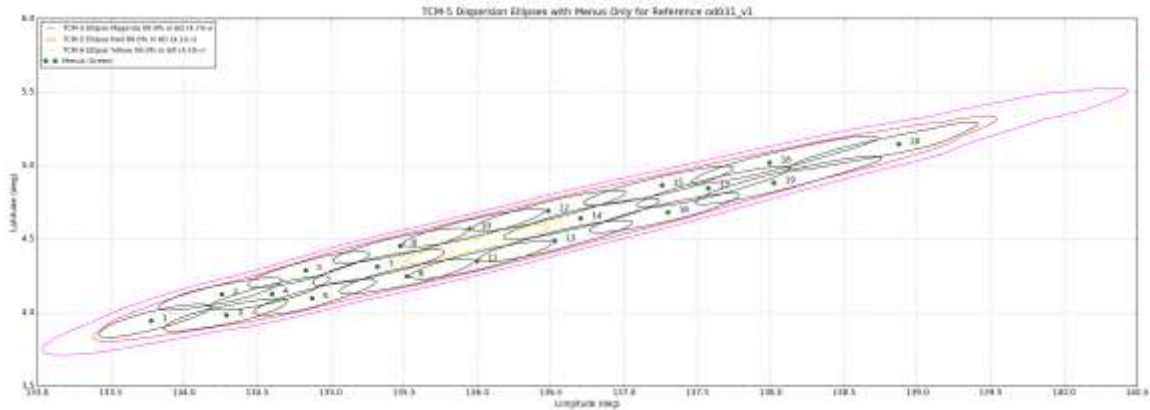


**Figure 9. Twenty TCM-6XM Menu Distribution.** A dispersion ellipse of  $\Delta V_y$  by  $\Delta V_z$  size in the Velocity Frame are distributed within the 99% TCM-5 dispersion ellipse.

Furthermore, using the combination of the two interpolations above, the result of applying a TCM-6XM  $\Delta V$  in the Velocity Frame to a TCM-5 sigma dispersion can be easily estimated to the landing dispersion without actually running DSENDS.\* Figure 10 below shows 100,000 randomly sampled TCM-5 dispersions corrected by one of the twenty TCM-6XM menu maneuvers. Thankfully, the spacecraft performed well and TCM-6XM did not have to be used in operations.

\* It took only about 45 minutes on one CPU to map them on to the surface in this way; actually propagating them via DSENDS would have taken about 35 CPU days.

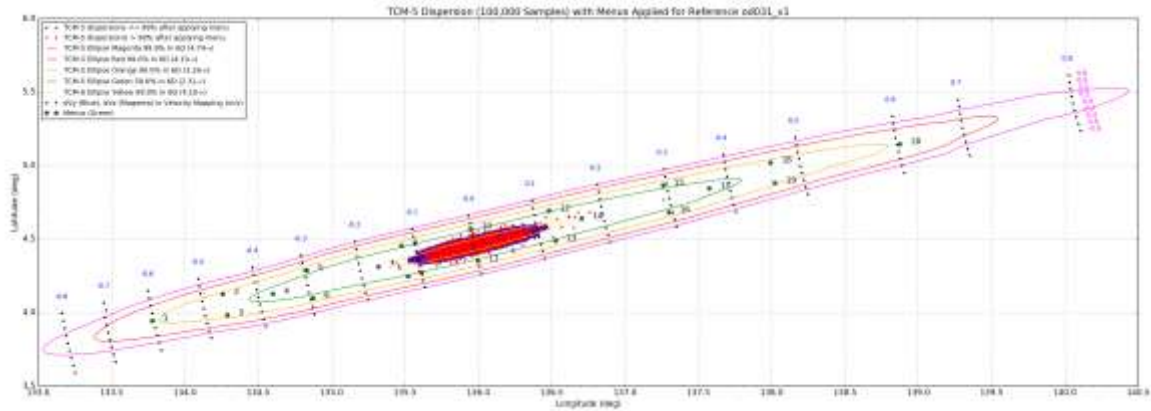


**Figure 10. Twenty TCM-6XM Menu Distribution.** A dispersion ellipse of  $\Delta V_y$  by  $\Delta V_z$  size in the Velocity Frame are distributed within the 99% TCM-5 dispersion ellipse.

## CONCLUSION

Through several Operational Readiness Tests (ORTs) the navigation and maneuver design tools were honed into final forms and the analysts were trained and prepared for the pace and expectations of operations. For the several months from Earth launch to Mars landing each TCM was dealt with one at a time, sometimes working on weekends, holidays, and nights. In the end, the InSight team encountered no major issues and was able to see InSight landed safely on Mars.

## ACKNOWLEDGMENTS

The research described in this paper was carried out at the Jet Propulsion Laboratory, California Institute of Technology, under a contract with the National Aeronautics and Space Administration. The authors would like to acknowledge the members of the InSight OD, EDL, and GNC teams who contributed to the analyses that are reported on in this paper. The authors also thank Roby Wilson and Ralph Roncoli for reviewing this paper. © 2018 California Institute of Technology. Government sponsorship acknowledged.

## REFERENCES

- <sup>1</sup> F. Abilleira, A. Halsell, M. Chung, K. Fujii, E. Gustafson, Y. Hahn, J. Lee, S. E. McCandless, N. Mottinger, J. Seubert, E. Sklyanskiy, and M. Wallace, "2018 Mars InSight Mission Design and Navigation Overview." 2018 AAS/AIAA Astrodynamics Specialist Conference, Snowbird, UT, August 19-23, 2018.
- <sup>2</sup> E. Bonfiglio, M. Wallace, E. Gustafson, E. Sklyanskiy, M. Chung, and D/ Kipp, "Atmospheric Impacts on EDL Maneuver Targeting for the InSight Mission and Unguided Mars Landers." 29<sup>th</sup> AAS/AIAA Space Flight Mechanics Meeting, Ka'anapali, HI, January 13-17, 2019.